

Reconciling atmospheric water uptake by hydrate forming salts

Bernadette Rosati,^{*,†,¶} Andreas Paul,^{†,§} Emil Mark Iversen,[†] Andreas Massling,[‡]
and Merete Bilde^{*,†}

[†]*Department of Chemistry, Aarhus University, Denmark*

[‡]*Department of Environmental Science, Aarhus University, Denmark*

[¶]*Faculty of Physics, University of Vienna, Austria*

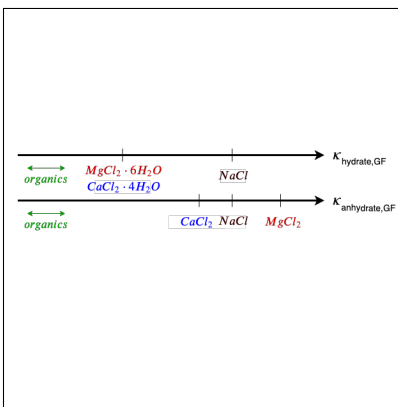
[§]*now at: Institute of Energy and Climate Research, Forschungszentrum Jülich, Germany*

E-mail: bernadette.rosati@chem.au.dk; bilde@chem.au.dk

Abstract

Magnesium and calcium chloride salts contribute to the global atmospheric aerosol burden via emission of sea spray and mineral dust. Their influence on aerosol hygroscopicity and cloud forming potential is important but uncertain with ambiguities between results reported in the literature. To address this, we have conducted measurements of the hygroscopic growth and critical supersaturation of dried, size selected nano-particles made from aqueous solution droplets of MgCl_2 and CaCl_2 , respectively, and compare experimentally derived values with results from state-of-the-art thermodynamic modelling. It is characteristic of both MgCl_2 and CaCl_2 salts that they bind water in the form of hydrates under a range of ambient conditions. We discuss how hydrate formation affects the particles' water uptake and provide an expression for hydrate correction factors needed in calculations of hygroscopic growth factors, critical supersaturations, and κ values of particles containing hydrate forming salts. We demonstrate the importance of accounting for hydrate forming salts when predicting hygroscopic properties of sea spray aerosol.

Graphical TOC Entry



Keywords

Hydrate forming salts, hygroscopicity, cloud activation, water activity

Atmospheric aerosols containing inorganic salts are ubiquitous in the Earth’s atmosphere and play a critical role in climate due to their interactions with sunlight and role in cloud formation.¹ Mineral dust is a major contributor to the atmospheric loading of inorganic salts and is mainly emitted from dry soils as a result of surface winds.^{2–5} Mineral dust is dominated by almost insoluble oxides and carbonates with low hygroscopicity.⁶ During atmospheric transit, surface reactions of these oxides and carbonates with acidic gases lead to the formation of MgCl_2 and CaCl_2 salts.^{7–9} These salts are soluble in water and thus directly impact particle water uptake.¹⁰ The oceans constitute another major emission source of inorganic salt, releasing so-called sea spray aerosols (SSA) through wave breaking at the ocean surface into the atmosphere.¹¹ SSA are comprised of a mixture of inorganic salts and organic species,^{11–13} where the relative ratio varies as a function of size.^{14–16} The hygroscopic nature of SSA is mainly driven by the inorganic fraction and although sodium chloride (NaCl) makes up the major inorganic compound in SSA by mass, recent work has shown that it is imperative to include the whole complexity of inorganic sea salt in assessment of its hygroscopicity¹⁷ and cloud forming potential.¹⁸ Rasmussen et al.¹⁹ pointed out that sea salt contains hydrate forming salts which affect volatility and hydrated forms of MgCl_2 and CaCl_2 have been proposed to be responsible for lowering the hygroscopic potential of sea salt compared to pure NaCl .¹⁷

While MgCl_2 is typically stable and solid in its hexahydrate state ($\text{MgCl}_2 \cdot 6\text{H}_2\text{O}$) at 298 K and relative humidities (RH) above 3%,²⁰ the hydration state of solid CaCl_2 at 298 K is much less clear. The number of water molecules associated with CaCl_2 may be 0, 2, 4 or 6 for humidities in the range 0–28%.²⁰ As a further complication the tetrahydrate ($\text{CaCl}_2 \cdot 4\text{H}_2\text{O}$) can exist in two allotropic forms with different solubilities²¹ and several of the hydrates may exist in meta-stable states.²²

Several recent studies have targeted the hygroscopicity and cloud activation potential of MgCl_2 and CaCl_2 salts^{6,9,23–26} revealing ambiguities in how to address and present the water uptake of hydrate forming salts. We here suggest a transparent and clear way of report-

ing hygroscopicity and cloud activation potential for hydrate forming salts of atmospheric relevance and provide a comparison to results from a state-of-the-art thermodynamic model.

We performed two series of experiments focusing on water uptake by nano-meter sized aerosol particles at sub- and supersaturated conditions of water vapor, respectively. These were complemented by bulk water activity measurements. A full description of the experiments and tabular values of experimental results are provided in the supplementary information (SI). In short, aerosol particles were generated from aqueous salt solutions ($\text{CaCl}_2(\text{aq})$ or $\text{MgCl}_2(\text{aq})$) using an atomizer and dried by dilution with dry clean air and passage through diffusion dryers ($\text{RH} < 10\%$). Water uptake was probed using a Humidified Tandem Differential Mobility Analyzer (HTDMA) and a Cloud Condensation Nucleus counter (CCNc).

The hygroscopic growth factors ($\text{GF}(\text{RH})$; defined as the ratio between humidified and dry particle diameter) were determined directly by HTDMA measurements and indirectly from measurements on bulk solution using a water activity meter. Figures 1a and 1c, present measured GFs as a function of RH for MgCl_2 and CaCl_2 particles generated from MgCl_2 and CaCl_2 aqueous solutions, respectively, with initial dry diameters of 200 nm. For comparison, experimental values reported in the literature deploying a similar aerosol generation technique and measurement principle for 100 nm⁹ and 50 nm²⁵ particles are shown. The results from this work confirm previously published values; at $\text{RH}=80\%$ Guo et al.⁹ report $\text{GF}=1.46$ and Park et al.²⁵ $\text{GF}=1.47$, while we find $\text{GF}=1.50$ for MgCl_2 , thus agreeing within the estimated uncertainty in GF of 3%. For CaCl_2 , the discrepancies are larger yielding GF values of 1.51,⁹ 1.48²⁵ and 1.69 (this study). All experimental studies show gradual increase in $\text{GF}(\text{RH})$ with increasing RH and gradual decrease with decreasing humidity. The lack of clear deliquescence and efflorescence indicates that the particles exist in an amorphous solid phase state after drying.⁹ Interestingly, clear deliquescence has been reported for larger (micro-meter sized) particles^{24,27,28} of MgCl_2 and CaCl_2 and measuring the mass of a bulk sample as function of RH.⁹ This confirms particle size to be a critical parameter in the phase state behavior of atmospheric aerosol particles.²⁹ If particle size is a determining parameter,

the actual size needed for crystal formation and thus deliquescence and efflorescence behavior of MgCl_2 and CaCl_2 particles is yet to be uncovered.

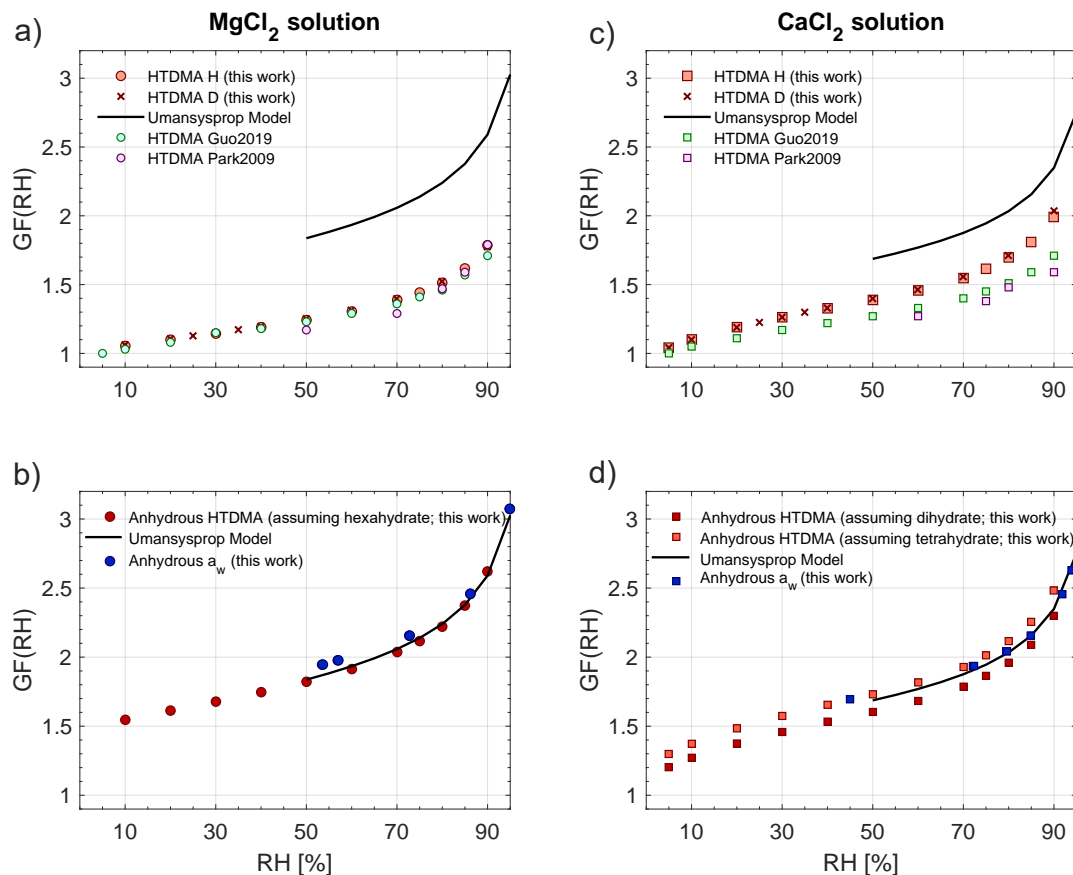


Figure 1: Hygroscopic growth factors vs. RH for dried particles made from aqueous solution of MgCl_2 and CaCl_2 salts. Panels a) and c) show experimental values from this work and literature.^{9,25} Regarding HTDMA results from this work, crosses indicate values recorded during dehydration (HTDMA D) while all other values stem from hydration branch measurements (HTDMA H). Panels b) and d) show HTDMA results (this work) after correction for hydrates along with GFs obtained from bulk water activity measurements (this work), derived following Zamora et al.³⁰ Solid lines represent model³¹ predictions for anhydrous salts ($D_{\text{dry}}=200$ nm).

Predictions from a state-of-the-art thermodynamic model (UManSysProp³¹) are also displayed in Fig. 1. The model runs were executed assuming that the particles consisted of MgCl_2 and CaCl_2 , respectively, in their anhydrous states. Figure 1a and 1c reveal a considerable gap between observed and predicted GFs. We argue that water bound as hydrates in the dry salts is responsible for this difference. It was recently pointed out that airborne

aqueous solution droplets containing MgCl_2 and/or CaCl_2 can form stable hydrates upon drying.¹⁹ The number of water molecules associated with the dried salt depends on temperature and RH^{20,22} and hence the hydration state of the salt dissolved in the aqueous solution is not necessarily representative for the hydration state of the dried nano-particles generated from the aqueous solution.

For MgCl_2 the stable hydration state at RH in the range 3-33% and a temperature of 298 K is $\text{MgCl}_2 \cdot 6\text{H}_2\text{O}$.²⁰ The dry particle diameter as selected by the first DMA in the HTDMA system at these conditions is thus not representative of an anhydrous particle but a particle containing $\text{MgCl}_2 \cdot 6\text{H}_2\text{O}$. To obtain the diameter ($D_p(\text{RH}, a)$) and growth factor ($\text{GF}(\text{RH}, a)$) of the anhydrous salt particle, we correct the selected dry diameter in the first DMA ($D_p(\text{RH}, h)$) to account for hydrate water by applying a hydrate correction factor (c_H):

$$\begin{aligned} D_p(\text{RH}, a) &= c_H \cdot D_p(\text{RH}, h), \\ \text{GF}(\text{RH}, a) &= \frac{\text{GF}(\text{RH}, h)}{c_H}, \end{aligned} \tag{1}$$

where $\text{GF}(\text{RH}, h)$ is the observed (hydrated) growth factor. As derived in the SI the hydrate correction factor c_H is calculated by assuming spherical particles with a specific molar mass (M) and density (ρ):

$$c_H = \left(\frac{M_a \cdot \rho_h}{M_h \cdot \rho_a} \right)^{1/3}. \tag{2}$$

Here the subscripts a and h refer to the anhydrous and hydrated salt, respectively. As seen in Fig. 1b, HTDMA and modeled data agree almost perfectly (within 1%) for MgCl_2 when the $\text{GF}(\text{RH})$ values are corrected for contributions of hydrate water. This result is further supported by the good agreement between GFs for the anhydrous salt derived from water activity (a_w) measurements (this work) following the procedure described in Zamora et al.³⁰

The hydration state of CaCl_2 in dried particles is more difficult to infer as several possibilities are plausible. Small changes in RH, e.g. from 9-21% to 21-28%, can change $\text{CaCl}_2 \cdot 4\text{H}_2\text{O}$

to $\text{CaCl}_2 \cdot 6\text{H}_2\text{O}$ ²⁰ at 298 K, and a change in temperature from 298 to 303 K can induce a hydration change from $\text{CaCl}_2 \cdot 6\text{H}_2\text{O}$ to $\text{CaCl}_2 \cdot 4\text{H}_2\text{O}$.^{20,32} It is thus challenging to access the hydration state of CaCl_2 particles generated by drying of aqueous solution droplets as in this work, in literature^{6,9,23,25,26} and in the atmosphere. Figure 1d shows $\text{GF}(\text{RH})$ for CaCl_2 corrected assuming dihydrate ($2 \cdot \text{H}_2\text{O}$) and tetrahydrate ($4 \cdot \text{H}_2\text{O}$) states. It is clear that a correction is needed to reach agreement with the model output for anhydrous salt particles but it is not possible to infer the actual hydration state as the best correlation depends on the actual RH. This result likely reflects that we cannot exclude that individual particles may contain several hydration states of the salt. Additionally, Fig. 1d shows $\text{GF}(\text{RH})$ values retrieved from a_w providing excellent agreement with model data. For completeness, $\text{GF}(80\%)$ was measured as a function of initial dried particle diameter (40-200 nm) for both salts and in all cases agreement with the model was only reached after application of the hydrate correction factors (see SI).

Table 1 provides hydrate correction factors (c_H) for the different hydration states of MgCl_2 and CaCl_2 . Since in the atmosphere hydrate forming salts are likely present in their hydrated state, modelled hygroscopic growth factors based on the assumption of anhydrous salts should be corrected to account for the effect of hydrates using c_H .

Table 1: Hydrate correction factors for the atmospherically relevant hydration states of MgCl_2 and CaCl_2 , assuming spherical particles at $T=298.15$ K. Densities and molar masses used for this calculation can be found in the SI.

Compound	c_H
$\text{MgCl}_2 \cdot 6\text{H}_2\text{O}$	0.68
$\text{CaCl}_2 \cdot 2\text{H}_2\text{O}$	0.87
$\text{CaCl}_2 \cdot 4\text{H}_2\text{O}$	0.80
$\text{CaCl}_2 \cdot 6\text{H}_2\text{O}$	0.74

The particle ability to act as cloud condensation nuclei (CCN) is also affected by the salt hydration state. Figure 2 shows critical supersaturation (SS_{crit}) vs. dry particle diameter for MgCl_2 and CaCl_2 particles, respectively. As in the case of the HTDMA experiments, the dried particle diameter likely represents the diameter of a particle containing hydrated

salts. The hydrate correction factor, introduced in Eq. 2 and presented in Table 1, can be used to calculate the diameter of the anhydrous particle from the diameter of the hydrated particle (and vice versa). SS_{crit} measured for dried particles made from $MgCl_2$ and $CaCl_2$ aqueous solutions, respectively, are in relatively good agreement with previous findings^{6,23,26} (Fig. 2a and c). For hydrated $MgCl_2$ particles with a diameter of 50 nm we find $SS_{crit}=0.57$ ($\kappa=0.34$ ³³), while Gaston et al.²³ found $SS_{crit}=0.48$ for the same size ($\kappa=0.47$). For hydrated $CaCl_2$ Gaston et al.²³ report $SS_{crit}=0.24$ for particles with a diameter of 75 nm ($\kappa=0.56$), while Sullivan et al.⁶ find $SS_{crit}=0.265$ ($\kappa=0.46$). We obtained $SS_{crit}=0.275$ ($\kappa=0.42$) which is in best agreement with Sullivan et al.⁶ (see Fig. 2b). The most striking feature is again the significant divergence in observed CCN activity of dried salt particles and model results assuming anhydrous salts. Both literature studies assumed that $CaCl_2$ particles were present in their dihydrate state, while $MgCl_2$ was in its hexahydrate state.^{6,23}

So called intrinsic κ values can be calculated as:²³

$$\kappa_{int} = \frac{\nu \cdot \rho_s \cdot M_w}{\rho_w \cdot M_s}, \quad (3)$$

where ν is the number of ions, ρ_s and ρ_w are the densities of solute and water and M_w and M_s are the molecular weights of solute and water. κ_{int} for $CaCl_2 \cdot 2H_2O$ is 0.68 while experimental results assuming $CaCl_2 \cdot 2H_2O$ are notably lower.^{6,23} Gaston et al.²³ accounted for solution non-idealities using the van't Hoff factor and report on this basis a κ value of 0.589 for $CaCl_2 \cdot 2H_2O$. This is closer to their experimental result (0.56) but still higher than results from Sullivan et al.⁶ and from this study.

Applying the hydrate correction factors to the dry diameters from our study yield the results presented in Fig. 2b and 2d. In case of $MgCl_2 \cdot 6H_2O$ we obtain excellent agreement with model data. In the case of $CaCl_2$ the tetrahydrate or hexahydrate hypothesis leads to the best agreement. In comparison, the HTDMA results where best agreement was obtained assuming dihydrate or tetrahydrates and could be caused by slightly differing RH when the aerosols were size selected. Nevertheless, the results emphasize that including some hydration

even if the precise state is not known still yields a smaller error than assuming anhydrous particles.

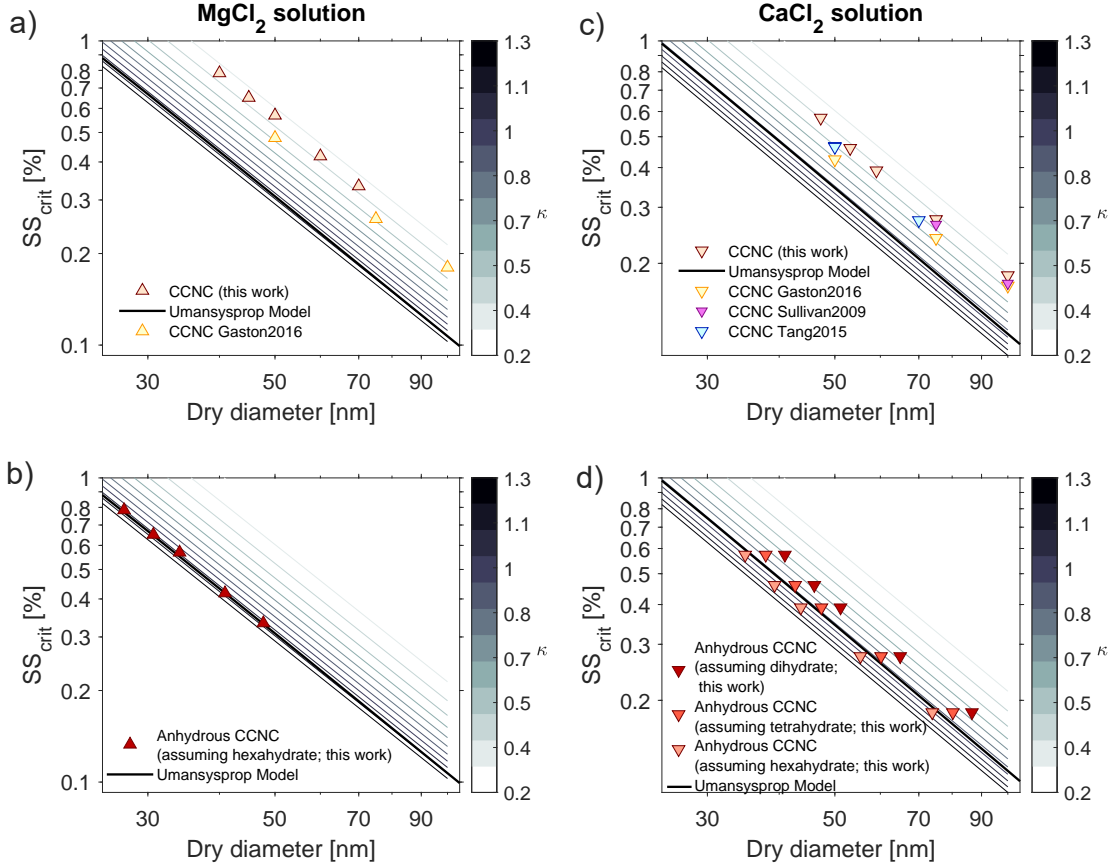


Figure 2: Critical super-saturations (SS_{crit}) as a function of size for $MgCl_2$ and $CaCl_2$ together with κ -isolines. Additionally, available literature data^{6,23,26} and model data are displayed. Panels a) and c) show data as directly obtained from the measurement, while b) and d) were corrected for hydrate contributions.

To reconcile hygroscopicity data gathered at sub- and supersaturated water vapour conditions, the hygroscopicity parameter κ ³³ is typically used. Figure 3 displays κ values obtained from HTDMA and CCNC measurements from this study and literature plotted vs. values calculated using the UManSysProp model. Generally, a large disagreement between experimental and modeled (assuming anhydrous particles) values is observed for both $MgCl_2$ and $CaCl_2$ (open symbols). Agreement between experimental and modelled κ values is obtained if particle diameters are modified to account for hydrate water following Eq. 2. We conclude

that the hydration state of MgCl_2 in dried salt nano-particles is 6 while for CaCl_2 hydration states in the range 2-6 are likely depending on drying procedure. Since results from subsaturated conditions suggest a hydration state of 2-4 and results from supersaturated conditions suggest a hydration state of 4-6, we suggest use of the tetrahydrate state if no firm knowledge on hydration state is available. Consistent with other studies for both organic and inorganic compounds,^{33,34} there is a significant difference in κ calculated from subsaturated (GF(RH)) and supersaturated (SS_{crit}) conditions: in the case of MgCl_2 the model results yield κ_{GF} of 1.89, while $\kappa_{\text{SS}_{\text{crit}}}$ is merely of 1.23, similarly a κ_{GF} of 1.38 and $\kappa_{\text{SS}_{\text{crit}}}$ of 0.97 were found for CaCl_2 .

For comparison, Fig. 3 additionally presents results for the notoriously hygroscopic NaCl salt, calculated from GF(RH) and SS_{crit} values (black symbols). It is evident that the anhydrous forms of MgCl_2 and CaCl_2 are actually extremely hygroscopic, with CaCl_2 reaching values close to those of NaCl ($\kappa_{\text{GF},\text{CaCl}_2}=1.38$, $\kappa_{\text{GF},\text{NaCl}}=1.49$) and MgCl_2 being much more hygroscopic than NaCl ($\kappa_{\text{GF},\text{MgCl}_2}=1.89$, $\kappa_{\text{GF},\text{NaCl}}=1.49$). When, however, considering the hydrated states of MgCl_2 and CaCl_2 , their κ reach comparable values around 0.5. It should be noted that NaCl is typically present in its anhydrous state except at temperatures below 273 K.²²

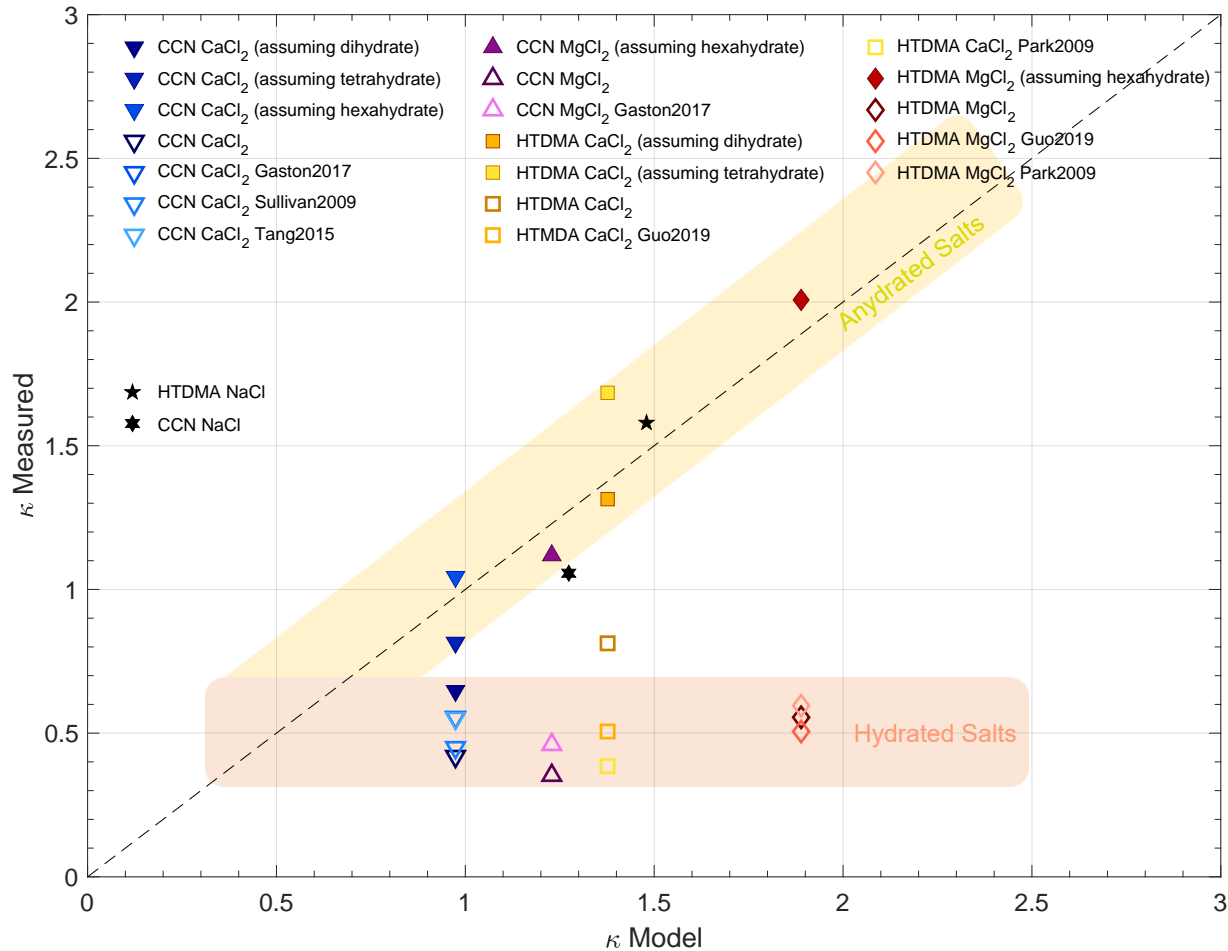


Figure 3: Hygroscopicity parameter κ : Comparison of κ values as calculated from HTDMA (taken at RH=90%) and CCNc (calculated as mean over all sizes, see SI) as well as literature data^{6,9,23,25,26} for MgCl_2 and CaCl_2 . The κ -Model data were obtained using the UManSysProp model. The dashed line represents the 1:1 line. All filled symbols were corrected for hydrates, while open symbols represent uncorrected data. Additionally, results for NaCl as measured and modeled from HTDMA and CCNc data are illustrated.

Figure 3 demonstrates the importance of hydrates for correct interpretation and prediction of hygroscopic growth and cloud droplet activation and shows that closure between experimental data and state-of-the-art model predictions can be achieved when hydrates are considered. These findings also underline that hygroscopicity of complex aerosols containing hydrate forming salts (such as sea salt) cannot be directly predicted by using models that combine properties of anhydrous salts as this approach leads to an overestimation of the hygroscopic growth as was shown in previous studies.¹⁷

181 The results from this study can be used to predict the hygroscopicity of oceanic sea
 182 salt. The major components of dried sea salt are NaCl, MgCl₂, Na₂SO₄ and CaCl₂.³⁵ As
 183 discussed above, NaCl is expected to be anhydrous at most ambient conditions. Na₂SO₄ has
 184 been shown to be present both in its anhydrous and decahydrate state.²² A previous study,
 185 however, found that suspended Na₂SO₄ microparticles are anhydrous.³⁶ This is supported
 186 by volatility experiments on dried mixed NaCl/Na₂SO₄ particles that did not evaporate
 187 at temperatures ranging from 50 to 300°C¹⁹ and GF measurements for Na₂SO₄ that were
 188 well comparable to theoretical calculations assuming anhydrites and Köhler theory.³⁷ Thus,
 189 Na₂SO₄ is treated as anhydrous in the following. Table 2 presents estimated GF, κ_{GF} and
 190 $\kappa_{SS_{crit}}$ values for two cases: (i) assuming sea salt consists of anhydrous salts only and (ii)
 191 considering hydrated MgCl₂ and CaCl₂ salts in sea salt. By applying a volume weighted
 192 mixing rule³³ sea salt GF_a of 2.38, $\kappa_{a,GF}$ =1.46 and $\kappa_{a,SS_{crit}}$ =1.21 are found. When includ-
 193 ing hydrated MgCl₂ and CaCl₂, GF_h of 2.14, $\kappa_{h,GF}$ =1.08 and $\kappa_{h,SS_{crit}}$ =0.89 are found. GF
 194 measurements of artificial sea salt particles yielded GF(90%)=2.09 and 2.19 (κ =0.96 and
 195 1.12) using a sea spray simulation tank and a nebulizer to generate sea salt particles, respec-
 196 tively,¹⁷ while κ =0.92 was found from CCNc measurements.³⁸ The herein calculated sea salt
 197 results including hydrated MgCl₂ and CaCl₂ are evidently in much better agreement with
 198 the sea salt experimental data than calculations based on the anhydrous salts alone.

Table 2: Calculations of the properties of sea salt considering (i) anhydrous salts only and (ii) hydrated forms of MgCl_2 and CaCl_2 . The volume fractions of the anhydrous salts ϵ_{va} are recalculated from the specifications by ASTM.³⁵ For case (i) anhydrous GFs, $\kappa_{a,GF}$ and $\kappa_{a,SS_{crit}}$ were calculated using the UManSysProp model. Hydrated GFs, $\kappa_{h,GF}$ and $\kappa_{h,SS_{crit}}$ were calculated assuming that NaCl and Na_2SO_4 were anhydrous, while $\text{MgCl}_2 \cdot 6\text{H}_2\text{O}$ and $\text{CaCl}_2 \cdot 4\text{H}_2\text{O}$ were present. The volume fractions of hydrated sea salt ϵ_{vh} were recalculated from the anhydrous case assuming volume additivity (see SI). GFs stem from measurements at $D_{dry}=200$ nm and $\text{RH}=90\%$, while $\kappa_{SS_{crit}}$ were calculated as mean over all measured sizes.

Anhydrous sea salt					Partly hydrated sea salt				
Compound	ϵ_{va} [%]	GF_a	$\kappa_{a,GF}$	$\kappa_{a,SS_{crit}}$	Compound	ϵ_{vh} [%]	GF_h	$\kappa_{h,GF}$	$\kappa_{h,SS_{crit}}$
NaCl	72.5	2.40	1.48	1.27	NaCl	53.8	2.40	1.48	1.27
MgCl_2	14.3	2.59	1.89	1.16	$\text{MgCl}_2 \cdot 6\text{H}_2\text{O}$	34.1	1.79	0.56	0.35
Na_2SO_4	9.7	1.93	0.72	0.88	Na_2SO_4	7.2	1.93	0.72	0.88
CaCl_2	3.5	2.35	1.38	0.92	$\text{CaCl}_2 \cdot 4\text{H}_2\text{O}$	5.0	1.99	0.81	0.42
mixture	100	2.38	1.46	1.21	mixture	100	2.14	1.08	0.89

In summary, the hygroscopic and cloud activation properties of MgCl_2 and CaCl_2 are dictated by their hydration state, which substantially lowers their ability to take up water. The behavior at sub- and supersaturated water vapour conditions differs remarkably, yielding higher κ values when calculated from the hygroscopic growth compared to when calculated from the SS_{crit} . When accounting for the hydration state of the salts, very good agreement can be achieved between measured and modeled data. This work demonstrates, that it is important to account for hydrate formation when predicting hygroscopic properties of complex aerosols containing hydrate forming salts, such as sea salt aerosols.

Acknowledgement

This research was supported by the Austrian Science Fund (FWF: J 3970-N36) and Aarhus University. The authors thank the Villum Foundation for support for instrumentation (HT-DMA and pre-humidifier) involved in this study.

Supporting Information Available

The Supplementary Information is available free of charge. Details of the calculation procedure for anhydrous particle size, experimental materials and methods as well as figures and tabular values for the hygroscopicity results from HTDMA, CCNc and water activity measurements are presented.

References

- (1) IPCC, *Climate Change 2013: The Physical Science Basis. Contribution of Working Group I to the Fifth Assessment Report of the Intergovernmental Panel on Climate Change.*; Cambridge University Press: Cambridge, United Kingdom and New York, NY, USA, 2013; Chapter SPM, pp 1–30, Stocker, T.F. and Qin, D. and Plattner, G.-K. and Tignor, M. and Allen, S.K. and Boschung, J. and Nauels, A. and Xia, Y. and Bex, V. and Midgley, P.M.
- (2) Tegen, I.; Fung, I. Contribution to the atmospheric mineral aerosol load from land surface modification. *Journal of Geophysical Research: Atmospheres* **1995**, *100*, 18707–18726.
- (3) Chou, C.; Formenti, P.; Maille, M.; Ausset, P.; Helas, G.; Harrison, M.; Osborne, S. Size distribution, shape, and composition of mineral dust aerosols collected during the African Monsoon Multidisciplinary Analysis Special Observation Period 0: Dust and Biomass-Burning Experiment field campaign in Niger, January 2006. *Journal of Geophysical Research: Atmospheres* **2008**, *113*.
- (4) Formenti, P.; Elbert, W.; Maenhaut, W.; Haywood, J.; Andreae, M. O. Chemical composition of mineral dust aerosol during the Saharan Dust Experiment (SHADE) airborne campaign in the Cape Verde region, September 2000. *Journal of Geophysical Research: Atmospheres* **2003**, *108*.

- (5) Nowak, S.; Lafon, S.; Caquineau, S.; Journet, E.; Laurent, B. Quantitative study of the mineralogical composition of mineral dust aerosols by X-ray diffraction. *Talanta* **2018**, *186*, 133 – 139.
- (6) Sullivan, R. C.; Moore, M. J. K.; Petters, M. D.; Kreidenweis, S. M.; Roberts, G. C.; Prather, K. A. Effect of chemical mixing state on the hygroscopicity and cloud nucleation properties of calcium mineral dust particles. *Atmospheric Chemistry and Physics* **2009**, *9*, 3303–3316.
- (7) Usher, C. R.; Michel, A. E.; Grassian, V. H. Reactions on Mineral Dust. *Chemical Reviews* **2003**, *103*, 4883–4940.
- (8) Santschi, C.; Rossi, M. J. Uptake of CO₂, SO₂, HNO₃ and HCl on Calcite (CaCO₃) at 300 K: Mechanism and the Role of Adsorbed Water. *The Journal of Physical Chemistry A* **2006**, *110*, 6789–6802.
- (9) Guo, L.; Gu, W.; Peng, C.; Wang, W.; Li, Y. J.; Zong, T.; Tang, Y.; Wu, Z.; Lin, Q.; Ge, M. et al. A comprehensive study of hygroscopic properties of calcium- and magnesium-containing salts: implication for hygroscopicity of mineral dust and sea salt aerosols. *Atmospheric Chemistry and Physics* **2019**, *19*, 2115–2133.
- (10) Tang, M.; Cziczo, D. J.; Grassian, V. H. Interactions of Water with Mineral Dust Aerosol: Water Adsorption, Hygroscopicity, Cloud Condensation, and Ice Nucleation. *Chemical Reviews* **2016**, *116*, 4205–4259, PMID: 27015126.
- (11) Lewis, E.; Schwartz, S. *Sea Salt Aerosol Production: Mechanisms, Methods, Measurements and Models*; American Geophysical Union, Washington DC, 2004; p 413.
- (12) Blanchard, D. C. The ejection of drops from the sea and their enrichment with bacteria and other materials: A review. *Estuaries* **1989**, *12*, 127–137.

- (13) Leck, C.; Bigg, E. K. Biogenic particles in the surface microlayer and overlaying atmosphere in the central Arctic Ocean during summer. *Tellus B: Chemical and Physical Meteorology* **2005**, *57*, 305–316.
- (14) Cochran, R. E.; Jayarathne, T.; Stone, E. A.; Grassian, V. H. Selectivity Across the Interface: A Test of Surface Activity in the Composition of Organic-Enriched Aerosols from Bubble Bursting. *The Journal of Physical Chemistry Letters* **2016**, *7*, 1692–1696.
- (15) Facchini, M.; Rinaldi, M.; Decesari, S.; Carbone, C.; Finessi, E.; Mircea, M.; Fuzzi, S.; Ceburnis, D.; Flanagan, R.; Nilsson, E. et al. Primary submicron marine aerosol dominated by insoluble organic colloids and aggregates. *Geophysical Research Letters* **2008**, *35*.
- (16) Salter, M.; Hamacher-Barth, E.; Leck, C.; Werner, J.; Johnson, C.; Riipinen, I.; Nilsson, E.; Zieger, P. Calcium enrichment in sea spray aerosol particles. *Geophysical Research Letters* **2016**, *43*, 8277–8285.
- (17) Zieger, P.; Väisänen, O.; Corbin, J.; Partridge, D.; Bastelberger, S.; Mousavi-Fard, M.; Rosati, B.; Gysel, M.; Krieger, U.; Leck, C. et al. Revising the hygroscopicity of inorganic sea salt particles. *Nature Communications* **2017**, *8*.
- (18) King, S.; Butcher, A.; Rosenoern, T.; Coz, E.; Lieke, K.; De Leeuw, G.; Nilsson, E.; Bilde, M. Investigating primary marine aerosol properties: CCN activity of sea salt and mixed inorganic-organic particles. *Environmental Science and Technology* **2012**, *46*, 10405–10412.
- (19) Rasmussen, B. B.; Nguyen, Q. T.; Kristensen, K.; Nielsen, L. S.; Bilde, M. What controls volatility of sea spray aerosol? Results from laboratory studies using artificial and real seawater samples. *Journal of Aerosol Science* **2017**, *107*, 134 – 141.
- (20) Kelly, J. T.; Wexler, A. S. Thermodynamics of carbonates and hydrates related to

heterogeneous reactions involving mineral aerosol. *Journal of Geophysical Research: Atmospheres* **2005**, *110*.

(21) Raj, G. *Phase Rule, 5th Edition*; GOEL Publishing House, Meerut, 2014; p 214.

(22) Lide, D. *CRC Handbook of Chemistry and Physics, 85th Edition*; CRC Press, Boca Raton, FL, 2005; p 2661.

(23) Gaston, C. J.; Pratt, K. A.; Suski, K. J.; May, N. W.; Gill, T. E.; Prather, K. A. Laboratory Studies of the Cloud Droplet Activation Properties and Corresponding Chemistry of Saline Playa Dust. *Environmental Science & Technology* **2017**, *51*, 1348–1356.

(24) Gupta, D.; Eom, H.-J.; Cho, H.-R.; Ro, C.-U. Hygroscopic behavior of NaCl-MgCl₂ mixture particles as nascent sea-spray aerosol surrogates and observation of efflorescence during humidification. *Atmospheric Chemistry and Physics* **2015**, *15*, 11273–11290.

(25) Park, K.; Kim, J.-S.; Miller, A. L. A study on effects of size and structure on hygroscopicity of nanoparticles using a tandem differential mobility analyzer and TEM. *Journal of Nanoparticle Research* **2009**, *11*, 175–183.

(26) Tang, M. J.; Whitehead, J.; Davidson, N. M.; Pope, F. D.; Alfarra, M. R.; McFiggans, G.; Kalberer, M. Cloud condensation nucleation activities of calcium carbonate and its atmospheric ageing products. *Phys. Chem. Chem. Phys.* **2015**, *17*, 32194–32203.

(27) Ha, Z.; Chan, C. K. The Water Activities of MgCl₂, Mg(NO₃)₂, MgSO₄, and Their Mixtures. *Aerosol Science and Technology* **1999**, *31*, 154–169.

(28) Cohen, M. D.; Flagan, R. C.; Seinfeld, J. H. Studies of concentrated electrolyte solutions using the electrodynamic balance. 1. Water activities for single-electrolyte solutions. *The Journal of Physical Chemistry* **1987**, *91*, 4563–4574.

(29) Cheng, Y.; Su, H.; Koop, T.; Mikhailov, E.; Pöschl, U. Size dependence of phase transitions in aerosol nanoparticles. *Nature Communications* **2015**, *6*.

- (30) Zamora, I. R.; Tabazadeh, A.; Golden, D. M.; Jacobson, M. Z. Hygroscopic growth of common organic aerosol solutes, including humic substances, as derived from water activity measurements. *Journal of Geophysical Research: Atmospheres* **2011**, *116*.
- (31) Topping, D.; Barley, M.; Bane, M. K.; Higham, N.; Aumont, B.; Dingle, N.; McFiggans, G. UManSysProp v1.0: an online and open-source facility for molecular property prediction and atmospheric aerosol calculations. *Geoscientific Model Development* **2016**, *9*, 899–914.
- (32) Ropp, R. *Encyclopedia of the Alkaline Earth Compounds, 1st Edition*; Elsevier, 2012; p 1216.
- (33) Petters, M. D.; Kreidenweis, S. M. A single parameter representation of hygroscopic growth and cloud condensation nucleus activity. *Atmospheric Chemistry and Physics* **2007**, *7*, 1961–1971.
- (34) Whitehead, J. D.; Irwin, M.; Allan, J. D.; Good, N.; McFiggans, G. A meta-analysis of particle water uptake reconciliation studies. *Atmospheric Chemistry and Physics* **2014**, *14*, 11833–11841.
- (35) D1141-98, A. *Standard Practice for the Preparation of Substitute Ocean Water*; ASTM International: West Conshohocken, PA, USA, 2013.
- (36) Tang, I. N.; Fung, K. H.; Imre, D. G.; Munkelwitz, H. R. Phase Transformation and Metastability of Hygroscopic Microparticles. *Aerosol Science and Technology* **1995**, *23*, 443–453.
- (37) Hu, D.; Qiao, L.; Chen, J.; Ye, X.; Yang, X.; Cheng, T.; Fang, W. Hygroscopicity of Inorganic Aerosols: Size and Relative Humidity Effects on the Growth Factor. *Aerosol and Air Quality Research* **2010**, *10*, 255–264.

329 (38) Nguyen, Q. T.; Kjær, K. H.; Kling, K. I.; Boesen, T.; Bilde, M. Impact of fatty acid
330 coating on the CCN activity of sea salt particles. *Tellus B: Chemical and Physical*
331 *Meteorology* **2017**, *69*, 1304064.